arXiv:1103.1565v1 [physics.atm-clus] 8 Mar 2011

Complete dynamics of H_2^+ in strong laser fields

J. Handt, S. M. Krause, and J. M. Rost

Max Planck Institute for the Physics of Complex Systems,

Nöthnitzer Straße 38, D-01187 Dresden, Germany

M. Fischer,* F. Grossmann, and R. Schmidt

Institut für Theoretische Physik, Technische

Universität Dresden, D-01062 Dresden, Germany

(Dated: July 26, 2019)

Abstract

Based on a combined quantum-classical treatment, a complete study of the strong field dynamics of H_2^+, i.e. including all nuclear and electronic DOF as well as dissociation and ionization, is presented. We find that the ro-vibrational nuclear dynamics enhances dissociation and, at the same time, suppresses ionization, confirming experimental observations by I. Ben-Itzhak *et al.* [Phys. Rev. Lett. **95**, 073002 (2005)]. In addition and counter-intuitively, it is shown that for large initial vibrational excitation ionization takes place favorably at large angles between the laser polarization and molecular axis. A local ionization model delivers a transparent explanation of these findings.

Even for nature's simplest molecule H_2^+, no full-dimensional description (including rotation of the nuclei) of the ionization dynamics has been given up to date. While in the early days important mechanisms of strong field ionization could be identified in calculations with frozen nuclei [1], it was shown subsequently that nuclear vibration does have a crucial influence on the ionization dynamics. Prominent effects include the washout of charge resonance enhanced ionization at specific internuclear distances (CREI) [2, 3] by vibrational motion [4, 5] as well as Lochfraß (internuclear separation dependent ionization) [6, 7]. For laser pulses much shorter than a typical rotational period it has been reasonably assumed that rotation can be neglected [8, 9]. However, recent theoretical work [10] has revealed the importance of rotation for the dissociation channel even for very short laser pulses. From a key experiment [11] it could be concluded that rotation and/or orientation is also relevant for ionization, which appears to be overestimated when the molecule remains aligned with the laser polarization.

All these findings can be put into a stringent perspective with the results from our present calculations taking all degrees of freedom into account. The mixed quantum-classical non-adiabatic quantum molecular dynamics (NA-QMD) method [12–14] which has enabled us to perform a full dimensional calculation is still approximate since it treats the nuclei classically. Hence, we have carefully assessed its validity for parameter regimes where accurate quantum calculations can be performed. In [9] dissociation and ionization of laser-aligned H_2^+ molecules were calculated and in [14] we have obtained vibrationally resolved angular distributions of dissociated fragments for laser parameters where ionization can be neglected. In both cases we have found quantitative agreement with appropriate quantum results, in the first case from a dimensionally reduced quantum approach [9], in the second case from full-dimensional quantum calculations, however restricted to dissociation [14]. Therefore, the mixed quantum-classical NA-QMD approach appears to be well suited to quantify ionization for H_2^+ including all degrees of freedom, for which no calculations exist so far.

Our starting point is the time-dependent electronic Schrödinger equation (atomic units are used)

$$\mathrm{i}\frac{\partial}{\partial t}\Phi(\mathbf{r},t;\{\mathbf{R}_A\}) = \left[\hat{T}_{\mathbf{r}} - \sum_{A=1}^{2}\frac{1}{|\mathbf{r}-\mathbf{R}_A|} + z\epsilon(t)\right]\Phi(\mathbf{r},t;\{\mathbf{R}_A\}), \tag{1}$$

which is solved in basis expansion self-consistently with Newton's equations of motion for the nuclei. Here, $\mathbf{R}_A$ $(A = 1, 2)$ and $\mathbf{r}$ denote the nuclear and electronic coordinates, $\hat{T}_{\mathbf{r}} = -1/2\nabla^2_{\mathbf{r}}$ the electronic kinetic energy, and $\epsilon(t)$ is the electric field of the laser. Details regarding the method and its numerical implementation can be found in [13, 14]. At the final time t_{f} the vibrationally resolved ionization (I) and dissociation (D) probabilities are constructed from probability densities along relevant nuclear trajectories,

$$P_{\mathrm{I}}(\nu) = 1 - Z_\nu^{-1} \sum_{i=1}^{Z_\nu} N[\mathbf{R}_i](t_{\mathrm{f}}) \tag{2}$$

$$P_{\mathrm{D}}(\nu) = Z_\nu^{-1} \sum_{i:R_i(t_{\mathrm{f}})>R_{\mathrm{D}}}^{Z_\nu} N[\mathbf{R}_i](t_{\mathrm{f}}), \tag{3}$$

where $N[\mathbf{R}](t)$ is the norm of the electronic wavefunction, which is a functional of the trajectory $\mathbf{R}(t)$ and a function of time. Its decrease in time, due to the presence of an absorber potential [13, 14], is a measure of ionization. Trajectories with final internuclear distance $R > R_{\mathrm{D}} = 10$ a.u. contribute to dissociation. Z_ν denotes the number of trajectories, sampled according to a micro-canonical distribution of a given initial vibrational state ν. With the molecule initially in its rotational ground state, the nuclear rotation angle θ is sampled uniformly in the interval $[0, \frac{\pi}{2}]$, where one has to take into account the additional weighting factor $\sin\theta_i(t_0)$ [14]. Complementary to the full dimensional calculations we have also performed dynamical calculations but with fixed nuclear orientation (frozen rotation) in order to study the influence of the rotational dynamics on the results.

We have determined vibrationally resolved ionization and dissociation probabilities for a linearly polarized laser pulse with an amplitude $\epsilon(t) = \epsilon_0 \sin^2(\pi t/T)\cos\omega t$ at a wavelength of 800 nm (corresponding to $\omega \approx 0.057$ a.u.), peak intensity of $I = 2\cdot 10^{14}\frac{\mathrm{W}}{\mathrm{cm}^2}$ (corresponding to $\epsilon_0 \approx 0.075$ a.u.) and total pulse length of $T = 50$ fs. Similar laser parameters were used in recent experiments [11, 15, 16].

Fig. 1a reveals that the full dimensional integral results for ionization (red circles, including rotational dynamics) agree quite well with those for frozen nuclear axis (dashed lines), where in both calculations the molecules are isotropically distributed in the beginning. This is understandable since over the length of the laser pulse (50 fs) during which ionization is possible the molecule hardly rotates. Dissociation, however, is much slower and its probability consequently deviates considerably from the result for frozen angles (black squares versus black dashed line). Only for weak binding at large ν dissociation happens even more quickly

than ionization so that $P_{\rm D}$ agrees with the frozen result. Moreover, this implies that beyond fragmentation saturation ($P_{\rm I} + P_{\rm D} = 1$, vertical dotted line), ionization is suppressed by dissociation according to $P_{\rm I}(P_{\rm D}) = 1 - P_{\rm D}$. Finally, the two maxima in $P_{\rm D}$ around $\nu = 4$ and $\nu = 11$ above the frozen probability are due to the well known dressed two- and one-photon states, respectively [14].

The corresponding probabilities for the molecule aligned with the laser polarization (Fig. 1b) differ quantitatively and qualitatively from the full dimensional analogs (Fig. 1a). Due to the much stronger ionization, fragmentation saturation sets in already near $\nu = 4$. Hence, for the aligned molecule ionization suppresses dissociation for high ν, according to $P_{\rm D}(P_{\rm I}) = 1 - P_{\rm I}$, in striking contrast to the real case (Fig. 1a). For the highest vibrational levels ionization decreases again, because there is a large probability that the molecules have an internuclear distance outside the strong ionization region (Fig. 2) when the laser reaches peak intensity. From Fig. 2 it is also clear why the full dimensional and laser aligned molecular response to the light pulse is so different: The coupling to the light changes considerably for different alignment angles and it is strongest in the aligned case where molecular enhancement mechanisms such as dressed state resonances and CREI are operative.

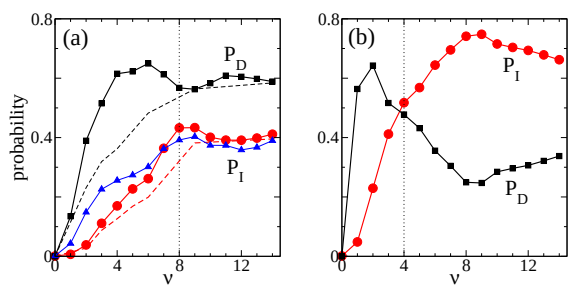

FIG. 1: (Color online) Ionization probability $P_{\rm I}(\nu)$ (red circles), and dissociation probability $P_{\rm D}(\nu)$ (black squares) for (a) initially rotationally cold molecules (isotropically orientated) and (b) *laser-aligned* molecules (see also [9]) as a function of the initial vibrational state ν. The dashed lines in (a) represent results for fixed nuclear orientation (frozen rotation). The vertical line denotes the vibrational level, above which fragmentation saturates, $P_{\rm D} + P_{\rm I} = 1$. Finally, the ionization probability based on the LIM (Eq. 6) is shown with blue triangles.

The angular distributions of dissociated and ionized fragments (Fig. 3) confirm what we have concluded from the integral probabilities of Fig. 1. For the ionization channel, the angular distributions follow roughly the behavior expected from geometric alignment. In

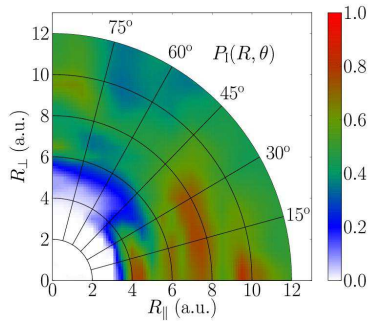

FIG. 2: (Color online) The ionization probability $P_I(\mathbf{R}) = 1 - N(\mathbf{R}, T)$ calculated for fixed nuclear positions with the parallel and perpendicular component $R_\parallel = R\cos\theta$ resp. $R_\perp = R\sin\theta$. Geometric alignment roughly manifests itself in increasing ionization probabilities towards the laser polarization direction. Near laser polarization direction clearly a region of strong ionization is visible, in particular the 1-photon-resonance at $R \approx 4.3$ a.u. as well as additional enhanced ionization maxima related to CREI.

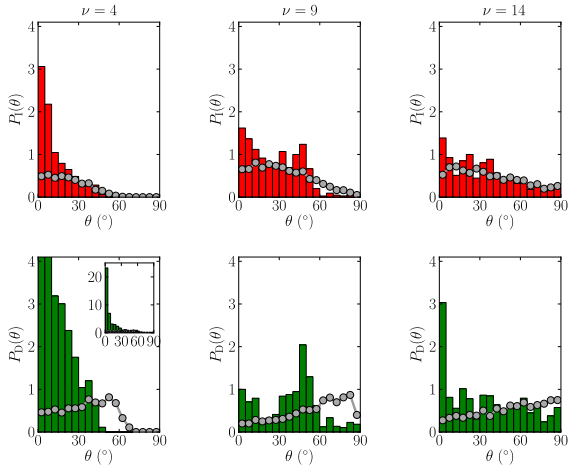

FIG. 3: (Color online) Angular distribution of fragments starting from vibrational H_2^+ levels $\nu =$ 4, 9, and 14 for ionization $P_I(\theta)$ (red bars) and dissociation $P_D(\theta)$ (green bars) from full dimensional calculations (cf. [14] for definition of $P_D(\theta)$, $P_I(\theta)$ analogous). The results calculated with frozen rotation are given with gray circles.

contrast, the angular distributions for dissociation from full dimensional and rotationally frozen calculations exhibit an opposite trend for increasing angle. Moreover, the strong alignment (for low and high ν) and anti-alignment for intermediate ν which has been explained and understood within the Floquet picture (e.g., [14]) is missing for frozen angles.

Summarizing the interpretation of the results so far it has become clear that a full dimensional approach is necessary to capture the dynamics adequately. Nevertheless, as the ionization probability depends exponentially on the laser intensity, a simplified dynamical description may be possible. In our case P_{I} from Fig. 2 is reduced ten times when using half the peak intensity which is also observed experimentally [11]. Hence, the full dynamical ionization should mainly be determined by the nuclear positions around peak intensity (25 fs into the pulse), dependent on the initial vibrational state as illustrated in Fig. 4a. To understand the influence of nuclear motion on ionization, we define the ionized nuclear density

$$\rho_{\mathrm{I}}(\mathbf{R}) = -Z_\nu^{-1} \sum_{i=1}^{Z_\nu} \int_0^{t_{\mathrm{f}}} \mathrm{d}t \; \dot{N}[\mathbf{R}_i](t) \; \delta(\mathbf{R} - \mathbf{R}_i(t)) \; , \tag{4}$$

which reveals preferential nuclear positions for ionization (Fig. 4b). Surprisingly, for large ν ionization proceeds favorably at large angles. It also corroborates the "naive" picture of Fig. 4a that ionization mainly takes place at the time of peak intensity and is therefore sensitive to the dynamically reached nuclear positions at this time.

To quantify this observation, we may assume that ionization happens instantaneously neglecting memory effects for nuclear motion in the approximation

$$\dot{N}[\mathbf{R}_i](t) \approx -\Gamma(\mathbf{R}_i(t), t) \; N[\mathbf{R}_i](t) \tag{5}$$

with an instantaneous local ionization "rate" $\Gamma(\mathbf{R}, t) = -\dot{N}(\mathbf{R}, t)/N(\mathbf{R}, t)$. Note that this assumption is not trivial, since the ionization of any trajectory in the swarm depends in principle on its whole time evolution. The instantaneous local ionization rate $\Gamma(\mathbf{R}, t)$ is calculated within the fixed-nuclei approximation using the same laser conditions as in the full dynamical calculations. This rate is not a simple function of time, internuclear distance and alignment angle, but also depends on the pulse shape of the laser. Inserting (5) into (4) leads to a local ionization model (LIM), where the ionized nuclear density takes the product form

$$\rho_{\mathrm{I}}^{\mathrm{LIM}}(\mathbf{R}) = \int_0^{t_{\mathrm{f}}} \mathrm{d}t \; \Gamma(\mathbf{R}, t) \; \rho(\mathbf{R}, t) \tag{6}$$

with the time-dependent nuclear density

$$\rho(\mathbf{R}, t) = Z_\nu^{-1} \sum_{i=1}^{Z_\nu} N[\mathbf{R}_i](t) \; \delta(\mathbf{R} - \mathbf{R}_i(t)) \; . \tag{7}$$

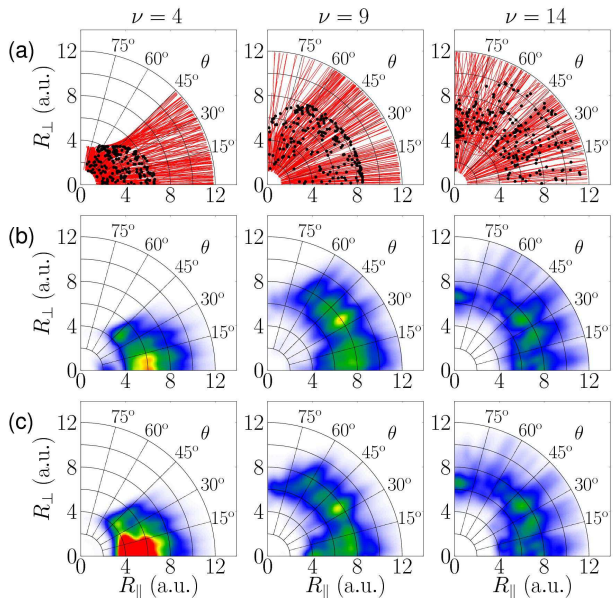

FIG. 4: (Color online) (a) Trajectories of fragmenting molecules (red lines) as well as nuclear positions at peak intensity (black dots) for exemplary initial vibrational levels ($\nu = 4, 9, 14$). (b) Corresponding exact ionized density $\rho_{\mathrm{I}}(\mathbf{R})$ and (c) ionized density in the LIM $\rho_{\mathrm{I}}^{\mathrm{LIM}}(\mathbf{R})$ (linear color scale). The nuclear coordinates are the same as in Fig. 2.

As one can see from Fig. 4c, the separation of nuclear dynamics and ionization according to (6) reproduces the full result Fig. 4b quite well and is in accord with the spirit of [17] with the difference that our ionization rates are extracted from the exact laser pulse.

Note, however, that the LIM overestimates ionization for low ν, which is due to the proximity of a 1-photon resonance close to $R \approx 4.3$ a.u. For higher ν the model reproduces that ionization takes place dominantly at intermediate angles as a consequence of dissociation dynamics [14]. The quantitative accuracy of the LIM (Fig. 1a, blue triangles) is overall comparable to the rotationally frozen result (dashed line), however LIM better reflects dynamical details, such as the influence of dressed state resonances.

A serious quantitative comparison with the experiment [11], which reveals one order of magnitude difference between total ionization and dissociation yield, requires Franck Condon averaging over initial vibrational levels and in addition focal volume and thermal averaging. While the former is a generally valid result, the latter depends on the exact conditions of individual experiments, which differ and are not trivial to quantify. Hence, we restrict ourselves to calculate full Franck-Condon averaged [18] angular distributions for ionization

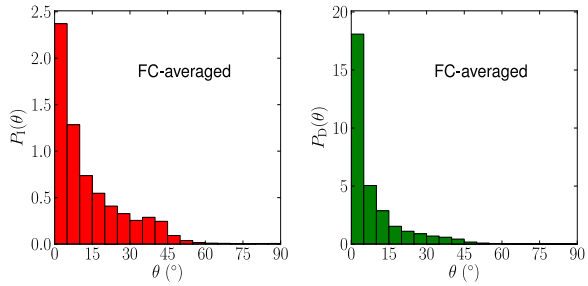

FIG. 5: (Color online) Franck-Condon averaged angular distribution for ionization ($P_{\rm I}(\theta)$) and dissociation ($P_{\rm D}(\theta)$).

and dissociation and discuss modifications due to volume averaging qualitatively. As one can see in Fig. 5, $P_{\rm D}(\theta)$ is more strongly aligned along the laser polarization than $P_{\rm I}(\theta)$ in seeming discrepancy with the opposite observation in the experiment. However, as noted in [11], the dynamics changes substantially with small changes in pulse length if the latter is close to the vibrational time scale which is the case here. Hence, the small differences in experimental and theoretical pulse length and shape may matter. Secondly, the spatial intensity profile of the laser will favor contributions of ionized fragments in the wings of the laser focus which originate dominantly from laser-aligned molecules. In the experiment [11] low laser intensities contribute considerably to the signal due to the width of the ion beam used. On the other hand, $P_{\rm D}(\theta)$ would broaden for large contributions from lower intensities (cf. the IDS procedure used in [19]). The total dissociation and ionization probabilities from our calculation, $P_{\rm I} = 0.13$ and $P_{\rm D} = 0.41$, reproduce the experimental trend, that ionization is considerably smaller than dissociation in sharp contrast to predictions from dimensionally reduced calculations.

In summary, we have presented a complete study of strong field ionization and dissociation of H_2^+. All nuclear and electronic degrees of freedom have been included in the framework of the mixed quantum-classical NA-QMD method whose applicability has been checked carefully in prior work by comparison to quantum results where available. It is worthwhile to note, that NA-QMD [12, 13] is also applicable to polyatomic many-electron systems [20].

We have found, that nuclear rotation enhances dissociation so that $P_{\rm D} > P_{\rm I}$ for H_2^+ under short pulses in agreement with the experiment [11] but in discrepancy with dimensionally reduced calculations. Furthermore, vibrationally resolved ionization $P_{\rm I}(\nu)$ is reasonably well

reproduced with frozen rotation, while $P_{\mathrm{D}}(\nu)$ is enhanced in comparison to frozen nuclear geometry with two maxima whose origin can be easily traced to one- and two-photon dressed states. The latter connection is almost completely lost in the dimensionally reduced result since due to the strong ionization, fragmentation saturation occurs already for $\nu > 4$ and leads to suppression of dissociation.

We conclude that full dimensional calculations are necessary for short pulses to obtain even qualitatively correct results. Nevertheless, a simplification arises in a local ionization model (LIM) from the separation of ionization and nuclear dynamics, taking advantage of the fact that ionization is fast, but happens dominantly at peak intensity, when nuclei have already moved. Finally, we could demonstrate that rotationally frozen dynamics is a good approximation when dissociation or ionization happens fast with respect to the rotational time scale. This is always the case for ionization with a 50 fs pulse and applies regarding dissociation to the highest vibrational levels, which dissociate before the molecule rotates substantially.

We gratefully acknowledge the allocation of computer resources from the ZIH of the TU Dresden and support by the DFG through Grants No. SCHM-957 and SCHU-1557.

* E-mail: Michael.Fischer@tu-dresden.de

[1] A. Giusti-Suzor *et al.*, J. Phys B **28**, 309 (1995).

[2] T. Zuo and A. D. Bandrauk, Phys. Rev. A **52**, R2511 (1995).

[3] G. N. Gibson, M. Li, C. Guo, and J. Neira, Phys. Rev. Lett. **79**, 2022 (1997).

[4] S. Chelkowski, C. Foisy, and A. D. Bandrauk, Phys. Rev. A **57**, 1176 (1998).

[5] I. Ben-Itzhak *et al.*, Phys. Rev. A **78**, 063419 (2008).

[6] E. Goll, G. Wunner, and A. Saenz, Phys. Rev. Lett. **97**, 103003 (2006).

[7] T. Ergler *et al.*, Phys. Rev. Lett. **97**, 103004 (2006).

[8] S. Chelkowski, T. Zuo, O. Atabek, and A. D. Bandrauk, Phys. Rev. A **52**, 2977 (1995).

[9] A. Kästner *et al.*, New J. Phys. **11**, 083014 (2009).

[10] F. Anis, T. Cackowski, and B. D. Esry, J. Phys. B **42**, 091001 (2009).

[11] I. Ben-Itzhak *et al.*, Phys. Rev. Lett. **95**, 073002 (2005).

[12] T. Kunert and R. Schmidt, Eur. Phys. J. D **25**, 15 (2003).

[13] M. Uhlmann, T. Kunert, and R. Schmidt, J. Phys. B **39**, 2989 (2006).

[14] M. Fischer *et al*, New J. Phys. (submitted).

[15] K. Sändig, H. Figger, and T. W. Hänsch, Phys. Rev. Lett. **85**, 4876 (2000).

[16] P. Q. Wang *et al.*, Phys. Rev. A **74**, 043411 (2006).

[17] H. A. Leth, L. B. Madsen, and K. Mølmer, Phys. Rev. Lett. **103**, 183601 (2009).

[18] D. Villarejo, J. Chem. Phys. **49**, 2523 (1968).

[19] P. Wang *et al.*, Opt. Lett. **30**, 664 (2005).

[20] T. Laarmann *et al.*, Phys. Rev. Lett. **98**, 058302 (2007).